ELSEVIER

International Journal of Pharmaceutics 200 (2000) 161–179

international journal of pharmaceutics

www.elsevier.com/locate/ijpharm

Structure and hydration properties of hydroxypropyl methylcellulose matrices containing naproxen and naproxen sodium

Ifat Katzhendler [a], Karsten Mäder [b], Michael Friedman [a,*,1]

[a] *Department of Pharmaceutics, School of Pharmacy, The Hebrew University of Jerusalem, PO Box 12065, Jerusalem 91120, Israel*
[b] *Department of Pharmaceutics, Free University, Kelchstrasse 31, 12169 Berlin, Germany*

Received 3 August 1999; received in revised form 31 January 2000; accepted 7 February 2000

Abstract

The present study was conducted to obtain a deeper insight into the mechanism of drug release from HPMC matrices. The microstructure, mobility, internal pH and the state of water within the gel layer of hydrated HPMC matrices (having different molecular weights) containing naproxen sodium (NS) and naproxen (N) were studied using Electron Paramagnetic Resonance (EPR), Nuclear Magnetic Resonance (NMR) and Differential Scanning Calorimetry (DSC) techniques. The study show that matrices composed of various viscosity grades of HPMC are characterized by similar microviscosity values in spite of the difference in their molecular weight. The NMR and DSC results led to the conclusion that higher molecular weights of HPMC are characterized by higher water absorption capacity and higher swelling. Analysis of non-freezable water in HPMC(K4M)–NS system revealed that addition of NS to solution increased the fraction of water bound to K4M + NS compared with the equivalent solutions without NS. The results suggest that the drug is participating in the crystallization of water and leads to the formation of a three dimensional network structure that decreases the freedom of water in K4M + NS samples. Calculation of the number of hydration shells showed that up to 2.2 layers are involved in HPMC-NS hydration compared to 1.5 layers for HPMC gel without NS. This was explained based on the different water ordering in the gel induced by NS as results of its absorption to polymer surface. Microviscosity values measured by EPR for K4M/N and K4M/NS hydrated matrices were found to be higher for K4M/N matrices, especially at initial stage of hydration. Mobile compartment calculations showed lower values for K4M/N compared with K4M/NS matrices. pH measurements by EPR revealed that incorporation of N to HPMC matrix led to lower internal pH value inside the hydrated tablet compared with NS. This behavior led to lower solubility of N which dictates its surface erosion mechanism, compared with NS matrix that was characterized by higher internal pH value and higher drug solubility. These properties of HPMC/NS increased chain hydration and stability, and led to drug release by the diffusion mechanism.

* Corresponding author. Tel.: + 972-2-6758664; fax: + 972-2-6757246.
E-mail address: mikef@cc.huji.ac.il (M. Friedman)
[1] Affiliated with the David R. Bloom Center for Pharmacy at the Hebrew University of Jerusalem.

0378-5173/00/$ - see front matter
PII: S0378-5173(00)00360-4

Keywords: Hydroxypropyl methylcellulose; Naproxen; Hydration; Electron paramagnetic resonance; Nuclear magnetic resonance; Differential scanning calorimetry

1. Introduction

Hydrophilic matrix sustained release dosage forms contain a therapeutic agent dispersed in a compressed water-swellable polymer matrix. When exposed to aqueous liquid, the surface polymer hydrates to form a viscous gel-layer (Melia, 1991). The gel layer forms a diffusional barrier that retards further water uptake and the release of the dissolved drug. Water-soluble drugs are released primarily by diffusion of dissolved drug molecules across the gel layer, whilst poorly water-soluble drugs are released predominantly by the erosion mechanism (Alderman, 1984). The contribution of each release mechanism to the overall drug release process is influenced both by drug solubility and also by the physical and mechanical properties of the gel barrier that forms around the tablet. Although outwardly simple, drug release from hydrophilic matrix systems is a complex phenomenon resulting from the interplay of many different physicochemical processes. In particular, the formation and physical properties of the hydrated surface barrier are an important determinant of subsequent behavior and drug release performance.

Despite the key role of the surface gel in the performance of these dosage forms, there have been few studies on the properties of this layer in-situ. Studies using cryogenic scanning electron microscopy (cryo-SEM) and other techniques have shown that a polymer concentration gradient exists across the gel layer (Melia et al., 1994) and that polymer in the outer regions is more homogeneously and extensively hydrated than the inner regions closer to the gel/core interface (Melia et al., 1990). The extent of polymer swelling and the hydration of the microstructure formed within the gel layer vary in accordance with polymer interaction with hydrating media (Melia et al., 1994; Hodsdon et al., 1995).

In previous studies the water mobility in the gel layer of plain matrices prepared from HPMC having different substitution level was studied using NMR technique (Rajabi-Siahboomi et al., 1996; Fyfe and Blazek, 1997). The diffusion of drug and water in a variety of solutions containing polymer gels were studied using pulsed-field-gradient spin-echo (PFGSE) NMR technique (Gao and Fagerness, 1995).

The present paper was conducted in order to get a deeper insight into the mechanism of drug release from HPMC matrices. The microstructure, mobility, internal pH and the state of water within the gel layer of hydrated HPMC matrices (having different molecular weights) containing naproxen sodium (NS) and naproxen (N) were studied using Electron Paramagnetic Resonance (EPR), Nuclear Magnetic Resonance (NMR) and Differential Scanning Calorimetry (DSC) techniques. Given its primary function as a diffusion barrier, the mobility of water and microviscosity of the gel layer is an important factor, which would be expected to influence polymer hydration, drug dissolution and release.

NMR relaxation and EPR spectroscopy are powerful techniques for studying in detail the structure, mobility, and hydration properties in various polymeric systems (Mathur-De Vre, 1979; Mäder et al., 1994). NMR longtitudal (T_1) and transverse (T_2) relaxation parameters are most useful in studying the ordering of water molecules in hydrogels. EPR spectroscopy is a noninvasive analytical technique which can provide unique information in the field of drug delivery using nitroxide radicals as model drugs (Stösser et al., 1995). The EPR spectra are sensitive to the nitroxide mobility. In addition to nitroxide mobility, pH measurements inside the delivery system are possible using specially designed nitroxides. The basic concepts of these techniques were reviewed in a previous paper (Katzhendler et al., 2000).

DSC is one of the most widely used analytical methods for studying the water of hydration in various polymers (Nakamura et al., 1983; Ohno et

al., 1983; Hatakeyama and Yamauchi, 1984; Roorda et al., 1988). It has been reported that different types of water are present in polymers and gels. At least two types of water of hydration have been identified. (I) Freezable water: Bulk-like water which melts at the normal melting point of pure water (0°C) and water weakly interacting with macromolecules which displays a lower melting point than pure water (< 0°C). (II) Non-Freezing water: Water strongly interacting with hydrophilic and ionic groups on the polymer and showing no freezing behavior.

2. Materials and methods

2.1. Materials

Hydroxypropyl methylcellulose having different viscosity grades (Methocel K100LV, Mn = 26 000; Methocel K4M, Mn = 86 000 and Methocel K100M, Mn = 246 000) were obtained from Colorcon, England. Naproxen sodium (NS) and naproxen (N) were obtained from Teva, Israel. 3-carboxy proxyl (PCA) was purchased from Sigma Chemicals, Israel. 4-amino-2,2,5,5-tetramethyl- 3-imidazolin-1-oxyl (AT) was obtained from Professor L.A. Grigoriev, Institute of organic Chemistry, Russian Academy of Sciences, Novosibirsk, Russia. Deuterium oxide (99.9%) was purchased from Aldrich Chemical, Israel.

2.2. Preparation of tablets

For release experiments, cylindrical tablets were prepared by direct compression of drug-polymer blends, using a laboratory press fitted with a 15-mm flat-faced punch and die set, and applying a pressure of 252 MPa (force if 4.45×10^4 N). All formulations contained 50% (w/w) drug. The final tablet weight in all formulations was 1 g.

2.3. Dissolution and erosion studies

2.3.1. Dissolution studies

The dissolution kinetics of the tablets was monitored using a tablet dissolution tester (model 7ST Caleva, USA). The USP basket method I was used. Rotation speed was 100 rpm and dissolution medium was 700 ml pH 7.4 (US Pharmacopea, 1985), maintained at 37°C. NS and N levels were monitored spectrophotometrically (Uvikon 930 Kontron spectrophotometer, Switzerland) at 271 nm. Dissolution studies were performed at least in triplicate for each batch of tablet.

2.3.2. Erosion studies

The erosion rates of HPMC matrices were determined gravimetrically. At various time intervals the tablets were removed from the baskets and dried for at least 24 h at 37°C until a constant weight was obtained. The percentage of tablet eroded was calculated from the weight loss of the tablets.

2.4. EPR measurements

2.4.1. Preparation of tablets

For EPR measurements, at 9.4 GHz, the nitroxide, 3-carboxy-proxyl (PCA), was dissolved in acetone, added to the polymer-drug blend and mixed thoroughly to allow even distribution of the spin label. The acetone was evaporated at room temperature. The final nitroxide concentration in the mixture was 4 mmol/kg. Tablets were prepared, using a laboratory press fitted with a 8 mm flat faced punch and die set, and applying a pressure of 886 MPa (force of 4.45×10^4 N). Tablet weight was 50 mg and the final tablet thickness was 0.8 mm. For internal pH measurements a pH sensitive nitroxide, 4-amino-2,2,5,5-tetramethyl-3-imidazolin-1-oxyl (AT) was used. The nitroxide was incorporated to the drug-polymer mixture using the procedure described above but using methanol as a solvent for AT. The final tablet weight was 100 mg, tablets' diameter was 8 mm and thickness 1 mm. Tablets were stored under dry conditions before EPR measurements were made.

2.4.2. Sample preparation for EPR measurements

2.4.2.1. Tablet hydration. Tablets, prepared as described previously, were hydrated in 10 ml pH 7.4, at R.T. At various time intervals the tablets were removed and handled without mechanical dam-

age. The water film at the surface was removed by blotting carefully with an absorbent paper. The tablets were loaded into an EPR teflon device (physical store, the Hebrew University of Jerusalem).

2.4.3. Measurements of EPR spectra

X-band (9.4 GHz) EPR spectra were recorded using a Jeol, JES-RE3X spectrometer with the following settings: field center, 329 mT; scan range, 7.5 mT; scan time, 1 min; time constant, 0.1 s; microwave power, 1–4 mW (depending on water content in sample); modulation amplitude, 0.1 mT. For the internal pH measurements, the EPR spectra were recorded using a surface coil equipped, 1.1 GHz spectrometer MT1 from Magnettech GmbH Berlin, Germany. The following parameters were used: field center, 41 mT; scan range, 5 mT; scan time, 1 min; time constant, 0.1 s; microwave power, 12 mW; modulation amplitude, 0.1 mT. All measurements were performed at R.T.

2.4.4. Spectra analysis

2.4.4.1. Line-width and line-shape analysis. Several experimental EPR spectra were a superposition of spectral contributions from mobile (solubilized) and immobile (nonsolubilized) nitroxide molecules. The analysis of the EPR spectra was performed by means of Bruker Winepr software (Version 2.11) in the following way. The immobile spectrum was adjusted in such a way that the outer lines of the immobile and experimental spectra overlapped. The mobile (solubilized) part of the experimental spectrum remained after subtraction of the simulated immobile spectrum. It has been shown that if the radical is placed a viscous fluid, the line width of each component ($M_I = +1,\ 0,\ -1$) has the form (Wertz and Bolton, 1972):

$$T(M) = \alpha + \beta M_I + \gamma M_I^2 \quad (1)$$

Coefficient α, is a constant term including all line-broadening effects which are the same for all hyperfine components. Coefficients β and γ depend on the anisotropy in g and of the hyperfine splitting, A, and on the mean tumbling rate (set by solvent viscosity), that is the molecular correlation time.

The line-width (α, β, γ parameters) and line-shape (lorentzian/gaussian ratio) simulations of the mobile part of the experimental spectrum were done using Winepr SimFonia program Version 1.25.

2.4.4.2. Determination of rotational correlation time of nitroxide in hydrated tablets. The immobile spectrum was subtracted from the EPR spectrum as described above. The rotational correlation time (τ_c) of the spin probe in the gel (subtracted spectrum) was calculated from the γ-parameter, using the equation (Nordio, 1976):

$$\tau_c = 8\gamma/b^2 \quad (2)$$

where γ is determined from line width simulations Eq. (1), $b = 2\pi(A_{zz} - a_0)$ and $a_0 = 1/3(A_{zz} + A_{yy} + A_{xx})$. a_0 is the isotropic hyperfine magnetic interaction between the unpaired electron and the nitrogen nucleus (a_{iso}). A_{xx}, A_{yy}, A_{zz} are the principal components of the hyperfine tensor (Berliner, 1976). A, b and γ values are expressed in MHz units.

The domain of validity of the formula used for analysis of the spin probe in the gel is $0.01\ \text{ns} < \tau_c < 300\ \text{ns}$.

2.4.4.3. Microviscosity calculations and determination of the mobile compartment in the tablet. The microviscosity values and the mobile compartment calculations of hydrated matrices were determined as described in our previous paper (Katzhendler et al., 2000).

2.4.4.4. Internal pH calculation

Determination of $2a_N$ values. The recorded EPR spectra were integrated and the distance between the first and third peak was used as the measure of $2a_N$, where a_N is the isotropic hyperfine splitting constant (a_{iso}).

Estimation of pH values inside the hydrated matrices. The $2a_N$ values of the recorded spectra were calculated and the pH was estimated relative to a suitable calibration curve.

Calibration curve-sample preparation. For calibration measurements, the nitroxides were dis-

solved in water (100 ml) or in commercial buffer systems (Schott GmbH, Germany) at a concentration of 1 mM. The pH value was adjusted by addition of 0.1 M HCl and 0.1 M NaOH using a magnetic stirrer. The pH was measured by means of a glass electrode (Schott GmbH) which was calibrated to the particular range by pH standards (Schott GmbH). Aliquates of 1 ml (microcentrifuge tubes, Scientific Plastic, USA) were taken and measured immediately at 1.1 GHz. The $2a_N$ values of the recorded spectra as function of pH were used as a calibration curve.

2.5. NMR relaxation studies

2.5.1. Preparation of tablets

For NMR relaxation studies, tablets were prepared by direct compression of drug-polymer blends, using a laboratory press fitted with a 3 mm flat-faced punch and die set, and applying a pressure of 1260 MPa (force of 8.90×10^3 N). All formulations contained 50% drug. The final tablet weight in all formulations was 30 mg.

2.5.2. Sample preparation

Five milimeter standard NMR tubes were filled with double distilled water and 11 tablets (arranged as a long cylinder) were inserted at once into the bottom of the tube using a rod. The T_1 and T_2 relaxation times of water as function of time were immediately recorded. The tablets formed a long cylinder inside the NMR tube with a length of approximately 4-cm.

2.5.3. T_1 and T_2 relaxation measurements

The T_1 relaxation time of water in the tablets was determined by an inverse recovery sequence (180°-τ-90°-acquire) (Derome, 1987). The T_2 transverse relaxation behavior of water in the tablets was determined using Carr–Purcell–Meiboom–Gill (CPMG) pulse sequence [90_x-(τ-180_y-τ)$_n$] (Derome, 1987). The T_1 and T_2 relaxation experiments were performed on a Bruker DRX 400 spectrometer as described in our previous studies (Katzhendler et al., 1999, 2000). All relaxation measurements were conducted at 25°C.

2.6. Self difussion coefficient (SDC) measurements

2.6.1. Preparation of gels for SDC measurements

HPMC (K100LV, K4M and K100M) solutions and gels in the concentration range 1-28.7% (w/w) were prepared with D_2O. NS concentration in the gel was fixed at level of 1% (w/v). SDC of NS was studied at HPMC (K100LV, K4M and K100M) concentration of 16.6% (w/w) while varying NS concentration (0.5, 1, 2, 3.5, 5, 7.5, 10% w/v) in the gel. HPMC gels especially at high polymer concentrations were difficult to load into 5-mm NMR tubes because of their high viscosity. Therefore, the gels were first loaded into 4-mm tubes (two-sided hollowed cylinder) having a length of 5 mm, after which the tubes were loaded into 5-mm standard NMR tubes.

2.6.2. Preparation of HPMC hydrated matrices for SDC measurements

For SDC measurements of hydrated matrices containing NS, the following concentrations were used: 1, 2.5,5,7.5 and 10% w/v NS (based on the final tablet volume). The tablets were formulated with Methocel K100LV, K4M and K100M. The total tablet weight was 30 mg and diameter was 10 mm. The tablets were hydrated in 20 ml solutions containing the same concentration of NS in D_2O. After full hydration of the matrices (3 h), the gels were loaded into NMR tubes as described in the previous section.

2.6.3. SDC measurements by NMR

The SDC measurements were performed in D_2O based on the method established by Tanner (1970). The pulsed field gradient stimulated spin-echo (STE) method was used (Tanner, 1970; Stilbs, 1987; Cotts et al., 1989). The pulse sequence consists of three pulses 90°-90°-90° which generates two stimulated field gradient pulses of duration, δ, during the τ periods. The integrated peak intensity I, of the species of interest is given by:

$$I = \frac{I_0}{2} e^{\frac{\tau_1}{T_1} - \frac{2\tau_2}{T_2} - (\gamma G\delta)^2 D\left(\Delta - \frac{\delta}{3}\right)} \quad (3)$$

where I and I_0 are the echo intensities with and without the field gradient, respectively; τ_1 is the time between the second and third pulses; τ_2 is the time between the first two pulses; T_1 and T_2 are the longtitudal and transverse relaxation times of the species, respectively; γ is the gyromagnetic ratio; G is the magnitude of the field gradient pulses; D is the self diffusion coefficient; δ is the gradient pulse length; and Δ is the time from the start of the first gradient pulse until the start of the second. The SDC, D, of water was extracted utilizing its 4.6-ppm (HDO/H_2O) resonance while the SDC of NS was extracted utilizing its 7–8 ppm resonance (from the aromatic moiety). Typically, experiments were performed keeping all parameters constant while incrementing G. The SDC was determined from the non-linear regression of the integrated peak intensity I against G^2.

The NMR experiments were performed on a Bruker DRX 400 spectrometer with BGUII gradient system capable of 56 G/cm. The gradient was calibrated using a cylindrical glass phantom sandwiched between two glass tubes and a hollow glass cylinder sandwiched between glass rods and recording the ^1H or ^2H NMR spectrum of the phantom immersed in solvent with the gradient on.

Standard 5-mm NMR tubes were used for all measurements. All measurements of diffusivity were conducted at 25°C. The temperature was determined using a standard methanol NMR thermometer.

2.7. DSC measurements

2.7.1. Calibration of DSC

The thermal analysis of the samples was performed using a differential scanning calorimeter (DSC, Mettler Toledo TA4000 with measuring cell DSC 30E, Switzerland). The DSC was calibrated with indium (melting point = 156.6°C) (Weast et al., 1986) having heat of fusion of 28.45 J/g.

2.7.2. Preparation of samples containing water for DSC measurements

Dried HPMC K4M samples were weighted accurately into aluminum samples pans. Before use in sample analysis, the aluminum pans were preheated to 100°C in the presence of water to minimize the reaction between the aluminum surface and water in the HPMC K4M samples. Various amounts of buffer (pH 7.4) were then added to HPMC K4M powder in the aluminum pans to obtain different ratios (w/w) of water to dry polymer. The pans were hermetically sealed, weighed and stored at room temperature for 3–5 days. Prior to the thermal analysis experiments, the sealed pans were re-weighed to check the seal. Samples with faulty seals, in which the amount of solutions decreased by more than 2% were discarded. The weight ratio of water per weight of HPMC K4M ($R_{W/K4M}$) was calculated by the following equation:

$$R_{W/K4M} = W_W / W_{K4M} \quad (4)$$

where W_W, grams of water (buffer) and W_{K4M}, grams of HPMC K4M.

In order to examine the effect of NS on the transition enthalpy of water in K4M samples, various amounts of 0.03, 0.05 and 0.1 g/ml NS solutions (prepared in buffer pH 7.4) were added to the dried HPMC K4M samples to obtain different ratios (w/w) of NS solution to HPMC K4M ($R_{NS/K4M}$).

2.7.3. Preparation of hydrated matrices for DSC analysis

50/50 K100LV/NS, K4M/NS, K100M/NS matrices were hydrated as described in the dissolution studies section. At specified times the matrices were removed, and samples were taken from the gelatinous outer portion of the matrices. The matrices were sliced in the center (parallel to the bases) and a sample was taken from the center of the core. The samples were weighted accurately into hermetically sealed aluminum pans for DSC analysis. The total amount of water in the sample was evaluated gravimetricaly. After DSC analysis, the pans were punctured and the water content was determined by heating the sample at 140°C until a constant weight was obtained. The weight ratio of water in the samples was calculated by dividing the total amount of water by the sample weight obtained after drying.

2.7.4. DSC analysis

DSC analysis of the samples were performed by cooling the samples from 20 to −50°C at cooling rate of 2.5°C/min, and then heating back to 20°C at the same rate. Heats of crystallization and melting were calculated from the peak areas of the exotherms and endotherms, respectively. The heat of melting in a sample was attributed to water were the melting enthalpy of pure water was 334 J/g (321 J/g for buffer 7.4).

2.7.5. Calculation of melting and crystallization enthalpy of water in K4M samples, NS solution and in hydrated tablets

Solutions containing 0, 0.03, 0.05 and 0.1 g/ml NS in buffer pH 7.4 were prepared. The melting (fusion) and crystallization enthalpy of water in buffer 7.4/K4M samples, NS solution, NS-solution/K4M samples and hydrated matrix tablets was calculated by dividing the enthalpy value obtained, by the weight fraction of buffer in the solution.

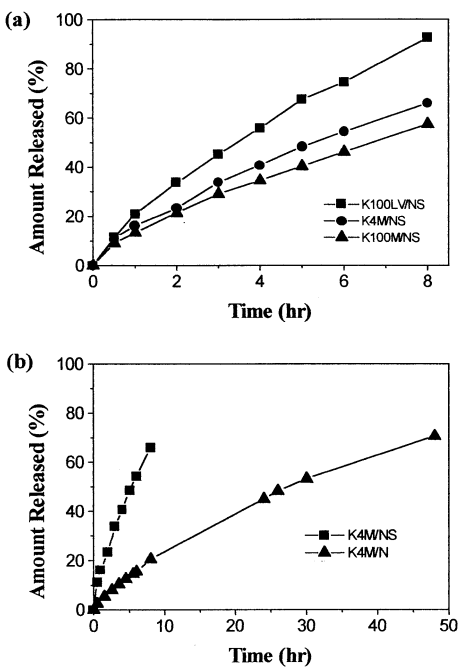

Fig. 1. The effect of (a) HPMC viscosity grade; and (b) drug solubility, on NS and N release from matrices containing 50/50 HPMC/drug.

To determine the melting enthalpy of water in HPMC matrices containing 50/50 K100LV/NS, K4M/NS and K100M/NS, the peak areas of the respective endotherms was divided by the total amount of water in the sample.

2.7.6. Calculation of amount of freezing and non-freezing water in K4M samples, NS solution and in hydrated tablets

To determine the amount of type I and type II water in K4M samples, NS solution and in hydrated tablets the following approach was used. The grams of freezable water (W_f) in the sample was determined by dividing the total heat of melting (J) by the experimental value of melting enthalpy of buffer pH 7.4 (J/g). From the grams of total water in the sample (measured gravimetrically) and the grams of freezable water (W_f) in the sample the grams of non-freezing water (W_{nf}) were calculated by the difference. The results were presented as grams of freezing or non-freezing water (W_f, W_{nf}) per gram of dry sample (w/w). For NS solutions/K4M samples the W_{nf} was devided by the grams of dry (K4M + NS). For calculation of moles non-freezing water bound per polymer repeat unit (PRU) the following data was used: Methocel K100LV: $M_n = 26\,000$, $DP_n = 140$; Methocel K4M: $M_n = 86\,000$, $DP_n = 460$; Methocel K100M = 246 000, $DP_n = 1280$.

3. Results and discussion

Fig. 1a presents the effect of HPMC viscosity grade on NS release from the matrix. Fig. 1b presents the effect of drug solubility on the release kinetics from HPMC K4M matrices (The solubility values for NS and N were found to be 450 and 5.2 mg/ml respectively, in pH 7.4, 37°C). The results obtained are in accordance with the data reported in the literature. The lowest viscosity grade of HPMC used (HPMC K100LV) provided the highest release rate compared to the higher viscosity grades (HPMC K4M, K100M) which showed similar release rates despite the variation in their molecular weight. The graphs also show that the release of low soluble drug (N) is lower compared with the high soluble drug (NS). The

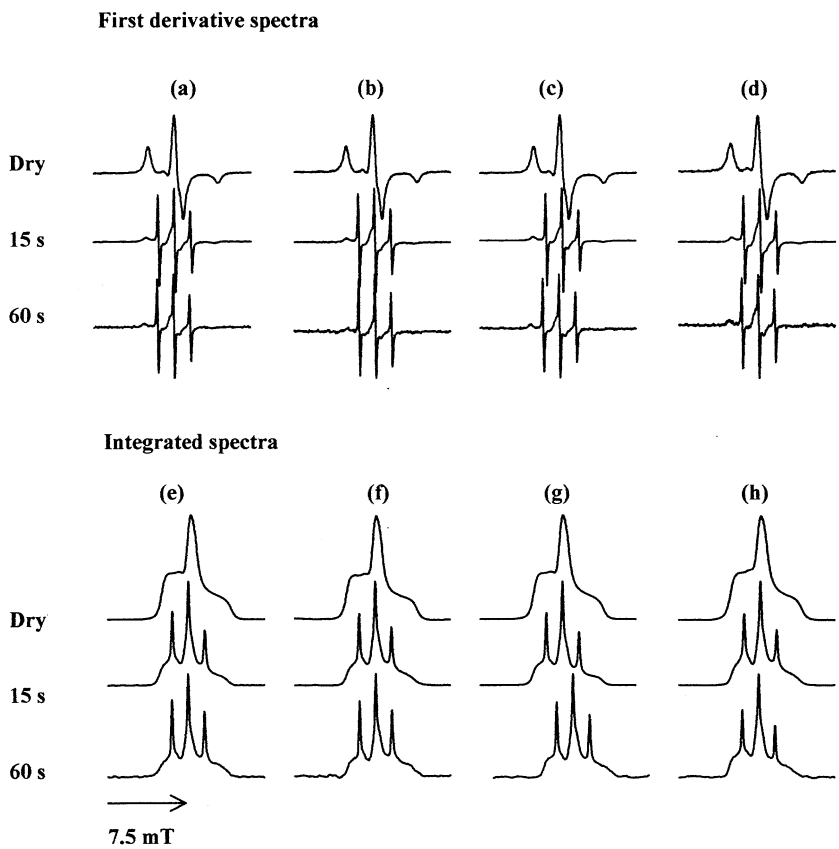

Fig. 2. EPR first derivative spectra of (a) 50/50 K100LV/NS; (b) 50/50 K4M/NS: (c) 50/50 K100M/NS; (d) 50/50 K4M/N. EPR integrated spectra of (e) 50/50 K100LV/NS; (f) 50/50 K4M/NS: (g) 50/50 K100M/NS; (h) 50/50 K4M/N.

release of the former is mainly controlled by the surface erosion mechanism (as revealed by similar values of drug release and matrix erosion) compared with the later (NS) in which drug release is controlled mainly by the diffusion mechanism (depending on polymer MW and concentration) (Alderman, 1984; Ford et al., 1987).

To study the influence of polymer MW and drug solubility on gel microstructure, microviscosity and hydration properties of the matrices, EPR spectra were recorded as function of hydration time. EPR studies performed at a frequency of 9–10 GHz (X-band) are limited to aqueous sample thickness less than 1 mm due to high non-resonant dielectric losses caused by water content in the sample. Therefore, our measurements were limited to thin tablets (< 1 mm) and to the initial hydration of the matrices, where matrix swelling was minimal. We assume that the changes in the recorded EPR spectra of the hydrated tablets can be used to characterize the gelation process occurring in the outer surface of the matrices. Fig. 2a–d presents the EPR spectra (first derivative) of hydrated matrices containing 50/50 HPMC/NS and HPMC/N of various viscosity grades at various time intervals. Fig. 2e–h presents the integrated spectra of the respective formulations. The integrated spectra can be used to estimate the amount of the mobile/immobile compartment because the contribution of the mobile species is more pronounced in the first derivative spectra due to the narrow line-width. The EPR spectra of the dry tablets indicate a high immobilization of the nitroxide, typical for solid samples with randomly oriented nitroxides. Exposure to buffer pH 7.4 induced modification of the microenvironment

inside the tablet. The EPR spectra indicated that water penetrated rapidly into the tablets leading to a spectral change from totally immobilized nitroxide to a spectrum which is dominated by mobile nitroxide solubilized in an environment with a low viscosity. The integrated EPR spectra of the hydrated matrices indicate a lower mobile compartment in matrices containing K4M/N (In higher immobile spectra the lines are much less intense compared to the mobile spectra due to line-broadening effect).

Table 1 summarizes the mobile compartment, rotational correlation time, microviscosity and α, β, γ parameters for the respective formulations. It was found that the mobile compartment was similar for the three viscosity grades containing NS, the mobile compartment was higher for K4M/NS compared with K4M/N matrix. Calculation of rotational correlation time and microviscosity values of the hydrated matrices revealed identical values for the formulations containing NS, irrespective of HPMC viscosity grade. The rotational correlation time and microviscosity values of formulation containing K4M/N was found to be higher compared to K4M/NS. The α, β, γ parameters show identical values for the three NS formulations irrespective of HPMC viscosity grade. The α, β, γ parameters were slightly higher for K4M/N indicating higher microviscosity values. At longer hydration times the α, β, γ parameters approached more closely zero implying increase of PCA mobility. The similar lorentzian/gaussian ratios for the four formulations (30/70 and 40/60 after 15 and 60 s, respectively) imply that the gel structure formed contain similar number of components. The contribution of gaussian spectral shape indicates the presence of several hydrophilic microdomains with distinct microviscosities. The lorentzian contribution increased at longer hydration times suggesting that the gel structure became more homogeneous.

Water diffusivity is also of interest in these systems because the water penetration rate determines the kinetics of the gel layer formation of a sustained release tablet and therefore, significantly affects drug dissolution and diffusion in the gel. In order to study the effect of HPMC viscosity grade on water and drug diffusion, NS and water SDC were examined in equilibrium-swollen gels with varied concentrations of HPMC. NS concentration was fixed at level of 1% (w/v). NS and water diffusivity, (D_{NS} and D_W), could be approximately described as an exponential function of the polymer concentration (w/w), C (Phillies, 1987, 1988):

$$D_{NS} = D_{NS}(0)\exp(-K_{NS}C) \quad (5)$$

$$D_W = D_W(0)\exp(-K_W C) \quad (6)$$

where $D_{NS}(0)$ and $D_W(0)$ are the SDC of NS and water respectively, extrapolated to infinite dilution. K_{NS} and K_W are constants indicative of the retarding effect of the polymer.

The K_{NS} and K_W values for NS and water were obtained by non-linear regression fit of the diffu-

Table 1
Mobile compartment (%), rotational correlation time (τ), microviscosity (cps), and α, β, γ parameters of hydrated HPMC matrices containing NS and N

Parameter	K100LV/NS		K4M/NS		K100M/NS		K4M/N	
	15 s[a]	60 s[b]	15 s	60 s	15 s	60 s	15 s	60 s
Mob.(%)	33.22	35.37	33.22	35.07	31.44	36.37	24.72	27.33
$\tau_{sec} \times 10^{11}$	4.70	3.13	4.70	3.13	4.70	3.13	5.61	3.39
Microviscosity (cps)	4.817	3.20	4.817	3.20	4.817	3.20	5.75	3.47
α	1.50	1.40	1.50	1.40	1.50	1.40	1.50	1.40
β	−0.12	−0.09	−0.12	−0.09	−0.12	−0.09	−0.13	−0.09
γ	0.18	0.12	0.18	0.12	0.18	0.12	0.215	0.13

[a] 15 s, Lorentzian/Gaussian ratio = 30/70 (for all four formulations).
[b] 60 s, Lorentzian/Gaussian ratio = 40/60 (for all four formulations).

Table 2
NS SDC values in different HPMC hydrated matrices equilibrated for 3 h (values-SDC $\times 10^6$ cm^2/s):

NS conc. (w/v)	K100LV/NS	K4M/NS	K100M/NS
1	2.15	2.37	2.66
2.5	1.82	1.97	2.11
5	1.42	1.72	1.80
7.5	1.28	1.38	1.61
10	1.05	1.16	1.41

sivity data and are reported here: K_{NS}(K100LV) = 9.32; K_{NS} (K4M) = 11.9; K_{NS}(K100M) = 12.28; K_W (K100LV) = 2.86; K_W (K4M) = 2.86; K_W(K100M) = 2.92.

NS diffusion in HPMC media showed little dependence upon HPMC viscosity grade, with tendency for lower diffusion values with increasing HPMC viscosity grades. Water diffusivities in HPMC media appeared to be indistinguishable among the three viscosity grades. This difference between drug and water diffusion can be explained based on the steric restriction imposed on the solute by a sieving mechanism. Since polymer macromolecules are less mobile than small solute or solvent molecules, the polymer acts as an obstructing stationary phase in the gel solution. Since the water molecule is small, the cooperative motion between obstructing stationary objects and diffusing species is unlikely as important as for large solute (e.g. drug) and the sieving mechanism of the polymer network is also less operative for water (Gao and Fagerness, 1995).

NS diffusion was additionally measured in gels containing 16.6% (w/w) HPMC and in water as function of NS concentration (C), using Eq. (5). The K values obtained are: K_{NS}(16.6% K100LV) = 6.19; K_{NS}(16.6% K4M) = 5.20; K_{NS}(16.6% K100M) = 4.08, K_{NS}(Water) = 7.25. The results indicate that NS diffusion is exponentially dependent upon its own concentration. Decreasing HPMC molecular weight (i.e. decreasing medium viscosity), increased the dependence of NS upon its concentration.

These results are in general agreement with the data reported by Gao et al for the diffusivity of adinazolam mesylate and water in HPMC gels containing K100LV, K4M and K15M. However in their study adinazolam diffusivity appeared to be indistinguishable among the three viscosity grades studied (Gao and Fagerness, 1995).

The data presented above refer to measurements in fixed concentrations of the polymer, however they do not reflect the effect of viscosity grade on drug diffusivity in the gel layer of hydrated matrices since the polymer concentration in the gel layer formed is controlled by the water absorption characteristics of the polymer. Since the different viscosity grades of the polymer may absorb different amounts of water, we have used the following approach in order to estimate drug diffusion in hydrated matrices: Tablets composed of HPMC (K100LV, K4M and K100M) containing different concentrations of NS were equilibrated with NS solutions in (D_2O) containing equivalent concentrations of NS. After full hydration of the tablets the gels were loaded into NMR tubes and NS diffusivity was measured. Table 2 summarizes the SDC values of NS obtained for the different HPMC gels. The results show higher diffusion of NS in higher viscosity grades of HPMC, implying higher water absorption capacity (higher swelling) and decrease of steric obstruction effect for higher MW of HPMC.

Fig. 3a and b present the T_1 and T_2 relaxation rates of water in HPMC/NS matrices having different MW. The results reveal that the T_1 and T_2 relaxation rates of water in the hydrated matrices are increased as function of time suggesting that there are considerable interactions between the water molecules and the polymer networks. The most probable binding sites of water molecules are the hydroxyl groups. The high T_1 relaxation rates of water protons in the hydrated matrices suggest that the water is less mobile compared with pure water. This can be interpreted in terms of the structure ordering of water molecules in gel networks. The graph show that T_1 water relaxation rates for K100M matrix are higher compared with matrices composed of K4M and K100LV indicating that the water molecules are interacting with the polymer to a greater degree. A similar trend was observed for T_2 relaxation rates however the relaxation kinetics was different. This difference may be attributed to the fact that T_2 relaxation is more strongly affected by

chain hydration (bound water). This can be anticipated since spin-spin (T_2) relaxation has other modes of relaxation in addition to those for spin-latice (T_1) relaxation; proton exchange processes and spin diffusion cause $1/T_2$ relaxation rate to be much higher than $1/T_1$ relaxation rate. The higher changes in proton relaxation rates for K100M matrices indicate higher swelling of the matrices compared with K4M and K100LV matrices. These findings are in agreement with our SDC measurements of hydrated matrices. Fig. 4a and b presents T_1 and T_2 relaxation rates of water in HPMC matrices containing NS and N. The graph shows that T_1 and T_2 relaxation rates of water are higher for HPMC(K4M)/NS matrices compared with HPMC(K4M)/N matrices. This implies higher chain hydration in matrices containing NS. These results are in agreement with the EPR data showing slower hydration of N matrices compared with NS matrices.

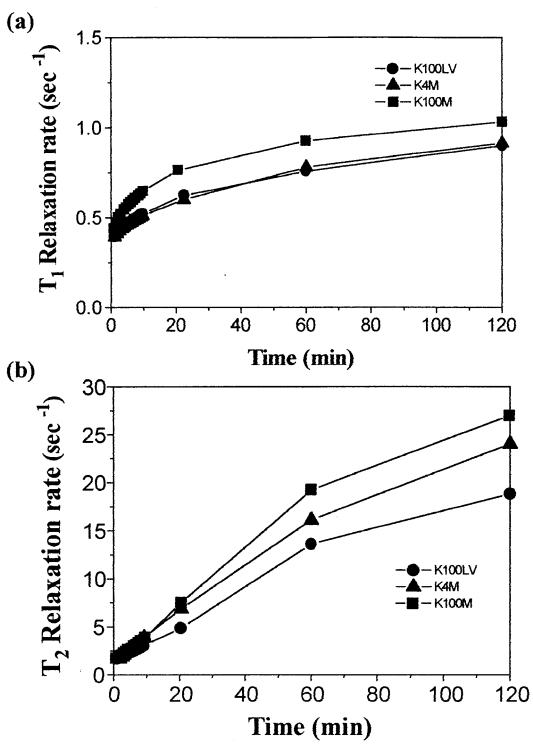

Fig. 3. (a) $1/T_1$; (b) $1/T_2$ relaxation rate of water in 50/50 HPMC/NS matrices containing different viscosity grades of the polymer.

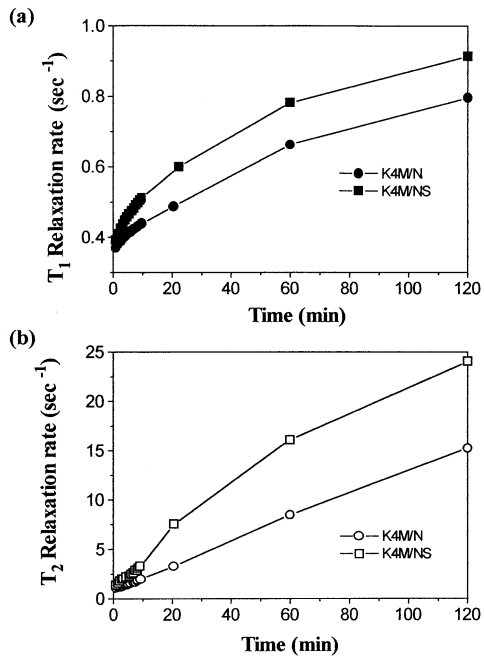

Fig. 4. (a) $1/T_1$; (b) $1/T_2$ relaxation rate of water in 50/50 HPMC/NS and 50/50 HPMC/N matrices.

To obtain a further insight on the relationship between drug/polymer properties and drug release kinetics, we have measured the pH inside the matrices using the pH sensitive spin probe, AT (Katzhendler et al., 2000), having $pK_a = 6.1$. The pH-induced changes of $2a_N$-hyperfine splitting of aqueous solutions of AT and the basic principle of pH measurements were presented in our previous study (Katzhendler et al., 2000). Fig. 5a–c presents the EPR spectra of HPMC(K4M)/NS, HPMC(K4M)/N and 100% HPMC(K4M) matrices exposed to buffer pH = 7.4 for different time intervals. The calculated $2a_N$ values, and the corresponding pH values calculated based on the calibration measurements, are presented in Table 3. It was found that the internal pH values in HPMC/N matrices were lower compared with HPMC/NS and 100% HPMC matrices. For the three formulations, the pH inside the hydrated matrices was lower than the hydrating buffer-pH 7.4. The observed decrease in pH suggests that the HPMC/N matrices are not able to preserve a neutral environment inside the tablets. The buffer

ions are not able to compensate the decrease in micro-pH inside the tablet induced by N. The increase of microacidity inside the tablet reduces N solubility and dissolution rate and lowers matrix hydration. These findings explain the slower release of N compared with NS from HPMC matrix. It should be emphasized that our measurements describe an average pH value inside the tablet. The formation of pH gradients inside the tablet with higher pH values in the outer hydrated layers of the tablet and lower values toward the center should be envisioned.

To explore water behavior in HPMC matrices in more detail the freezable and non-freezable water were analyzed using DSC. Fig. 6a shows the cooling curve of HPMC K4M with various water contents. When the weight ratio ($R_{W/K4M}$) of buffer in the samples was 0.516 (g/g) a peak similar to the peak of purified water was observed with an onset temperature of -34°C. In contrast a peak was observed with an onset temperature of -18°C for buffer solution. The depression of about 20°C in the crystallization temperature of water, compared with the melting temperature (Fig. 6b), is explained by the supercooling effect (Angell and Tucker, 1973).

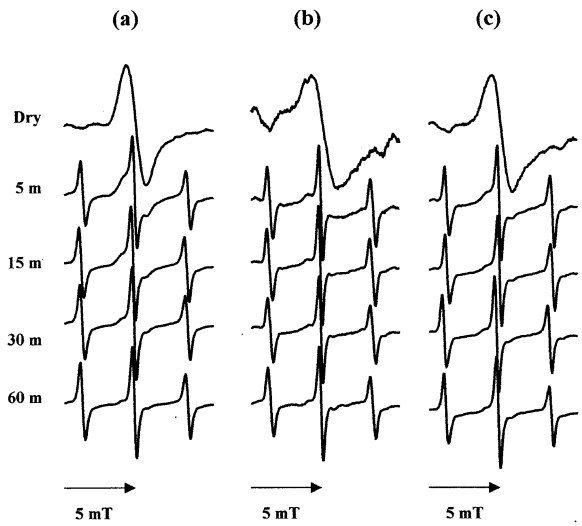

Fig. 5. 1.1 GHz EPR spectra of (a) 50/50 K4M/NS; (b) 50/50 K4M/N; (c) 100% K4M.

Table 3
Internal pH values of hydrated matrices containing 100% HPMC(K4M), 50/50 HPMC(K4M)/NS, 50/50 HPMC(K4M)/N (the values refer to hydration time; 5–60 min)

Formulation	$2a_N$-hyperfine splitting	pH
100% HPMC	3.139–3.145	6.7–6.9
50/50 HPMC/NS	3.139–3.145	6.7–6.9
50/50 HPMC/N	3.041–3.048	5.5–5.7

Fig. 6b shows the heating curves of HPMC K4M samples containing buffer. Similar to the cooling curves (Fig. 6a), as the water fraction decreased, the onset temperature and area of the endothermic peak decreased and this peak became broader. It was suggested that this fronting of the thermograms is due to the overlapping of endotherms of free-freezing and loosely bound-freezing waters (Joshi and Topp, 1992). The decrease observed in the onset temperature suggests an interaction of water with HPMC K4M. Table 4 summarizes the results for the amount buffer pH 7.4 added per HPMC K4M ($R_{W/K4M}$) (g/g) for the corresponding thermograms. The table also lists the onset temperatures for the melting of water in these samples, the percent of freezing and non-freezing water, and the amount of non-freezing water per polymer (w/w). Increasing $R_{W/K4M}$ increased the fraction of freezable water and correspondingly the fraction of non-freezable water decreased. Calculation of moles of water bound per polymer repeat unit (PRU) revealed that an average of 5.24 molecules of non-freezing water are bound to each PRU of HPMC (K4M).

Table 5 presents the effect of NS concentration in solution on the non-freezing water in K4M + NS samples. Since NS may also affect the melting enthalpy of water, this effect was first examined in NS solution. It was found that increasing NS concentration in solution marginally affected the melting enthalpy of water. The enthalpy values were within deviation of 4.2%, up to NS concentration of 0.1 g/ml. However in K4M/NS system increasing the concentration of NS in solution increased the amount of water bound to K4M + NS (Table 5).

The changes in HPMC hydration were calculated using the following approach:

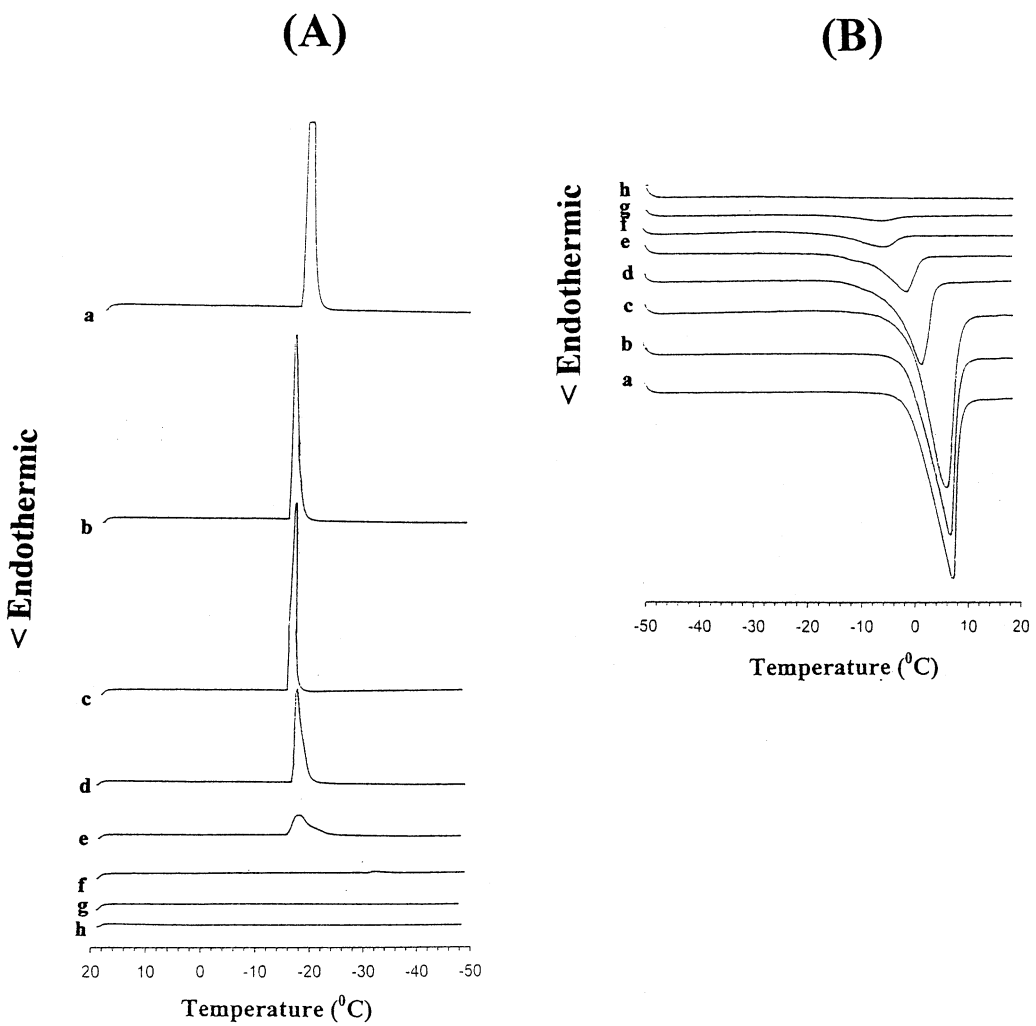

Fig. 6. DSC (A) cooling; and (B) heating curves of K4M samples with various weight fraction of buffer pH 7.4. $R_{W/K4M}$: (a) buffer 7.4; (b) 9.33; (c) 4.65; (d) 2.00; (e) 1.01; (f) 0.516; (g) 0.444; (h) 0.186.

The number of water molecules bound to HPMC K4M were calculated based on the difference between the specific partial volume (0.717 cm^3/g) and the van der Waals volume (0.440 cm^3/g) of HPMC. The van der Waals volume was calculated based on the additive contribution of the atomic groups comprising the polymer (Bondi, 1968). It was found that 2.87 water molecules are bound per PRU of HPMC K4M. Since HPMC contains three hydroxyl groups per PRU, it can be concluded that 1 water molecule is bound per each hydroxyl group in the first hydration layer.

In contrast, it was found (based on DSC data) that 5.24 water molecules are bound per PRU of HPMC K4M implying that more than one hydration shell is involved in HPMC hydration. The number of hydration shells of HPMC were calculated based on volumetric considerations, which depends on the molecule shape. For cylinder geometry, the ratio between the number of water molecules in the $n+1$ and n hydration shell is

Table 4
Amount of buffer 7.4 per HPMC K4M in the sample, melting point of water in hydrated HPMC K4M, percent of freezing and non-freezing water and amount of water bound per HPMC K4M

Buffer 7.4 (mg)	K4M (mg)	$R_{W/K4M}$ [a]	Onset Temp., °C	Freezing water (%)	Non-freezing water (%)	Non-freezing water/K4M (g/g)
2.087	11.30	0.186	–	0	100	0.186
3.86	11.13	0.347	−15.1	10.45	89.55	0.310
4.55	10.24	0.444	−14.4	22.68	77.32	0.343
5.37	10.40	0.516	−14.1	30.06	69.94	0.361
7.84	7.79	1.01	−13.3	54.68	45.32	0.456
10.14	5.06	2.00	−11.2	74.37	25.63	0.513
10.99	2.36	4.65	−5.5	89.18	10.82	0.504
19.32	2.07	9.33	−1.5	94.66	5.34	0.498

[a] Buffer 7.4 (mg) added per K4M (mg).

1.45. Based on this the number of hydration shells in HPMC gel was found to be 1.5.

The higher HPMC hydration can be understood as following: The DSC measurements were done in concentrated HPMC solutions in which HPMC forms an entangled gel network. The hydration of the gel is higher than polymer in dilute solution in which hydration is confined to the first hydration layer (2.87 water molecules per PRU). This enhancement could result from closely located polar (hydroxyl) groups of HPMC in the entangled gel favoring solvation via the formation of water networks which involve water molecules from the second coordination spheres. In such networks, a water molecule may simultaneously form hydrogen bonds with two or more polar groups on the polymer surface, thereby becoming highly immobilized. For low molecular mass compounds it was shown that the hydration of a polar group depends on its proximity to other polar groups (Kharakoz, 1991; Chalikian et al., 1994). The hydration of a single polar groups (separated from other polar groups by five or more covalent groups) was found to be low (Kharakoz, 1991). However, when polar groups within a solute molecule are situated sufficiently close to each other (separated by three or less covalent bonds) than it was postulated that each adjacent water molecule can, in principle, form simultaneously two hydrogen bonds with neighboring polar groups (Kharakoz, 1991; Chalikian et al., 1994). Consequently, the hydration of each group within two closely polar groups increases. By extension, in the polymer in the entangled state were there are many closely located polar groups, a water molecule can simultaneously form hydrogen bonds with more than two neighboring polar groups, thereby becoming highly immobilized.

Table 5
The effect of NS concentration in solution (buffer 7.4) on the amount of bound water per HPMC K4M + NS and on the number of hydration shells

Ratio[a]	Non-freezable water/K4M + NS (g/g)			Number of hydration shells		
	0.03 g/ml NS	0.05 g/ml NS	0.1 g/ml NS	0.03 g/ml NS	0.05 g/ml NS	0.1 g/ml NS
0.605	0.406	0.397	0.387	1.32	1.30	1.27
1.00	0.489	0.472	0.470	1.53	1.49	1.48
2.04	0.645	0.624	0.625	1.92	1.86	1.87
4.51	0.813	0.752	0.788	2.23	2.13	2.19
8.49	0.840	0.756	0.769	2.28	2.13	2.16

[a] NS solution (mg) added per K4M (mg).

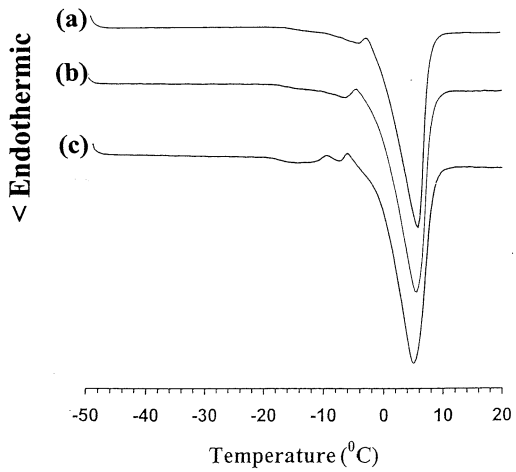

Fig. 7. DSC thermographs of K4M/NS samples (a) 0.03 g/ml; (b) 0.05 g/ml; (c) 0.1 mg/ml NS. $R_{NS/K4M} = 4.51$.

Furthermore, such highly immobilized water molecules on the polymer polar surface may, in turn, form hydrogen bonds with water from the second hydration shell, thus facilitating the formation of water networks. In such a scenario, these highly immobilized water molecules in the first hydration shell, act in some respect, as pseudopolar groups on the polymer surface, which facilitate the involvement in polymer hydration of water molecules from a second and even, possibly, a third coordination sphere.

When increasing NS concentration in solution an increase of the non-freezing water of HPMC K4M + NS was found. It should be emphasized that the hydration properties describe an average behavior of HPMC + NS. We calculated the number of hydration shells of this system based on the considerations described for HPMC gel, the number of hydration shells are summarized in Table 5. It can be seen that the number of hydration shells increased to 2.2 (at the highest NS concentration). These results can be interpreted based on the hydration theory described and discussed above.

The number of NS molecules per PRU of the polymer was calculated. The number of molecules per PRU was found to be less than 0.3, except for the highest concentration of NS (0.1 g/ml) at the highest NS solution/HPMC ratio (8.49) in which the value was 0.6. It has been suggested that large planar aromatic ions are polarizable and readily absorb to methylcellulose surface (Touitou and Donbrow, 1982). Therefore this system may promote the formation of deep polarized multilayers of adsorbed water. When NS is present in solution its hydration is low, however when added to the polymer, it alters the hydration structure of the NS-HPMC gel. The drug molecules, which contain a polar carboxyl group, are absorbed onto the polymer, adjacent to the polymer polar groups and thereby the system hydration increases significantly. This can be interpreted based on the theory described above which increases water immobilization in adjacent polar groups.

The graph shape of K4M-NS samples show a faint endothermic peak followed by an exothermic peak (in some cases) below 0°C (Fig. 7). The result suggest that the drug is participating in the crystallization of water which leads to the formation of a three dimensional network structure that decreases the freedom of water in K4M + NS samples. The faint endothermic peak and the exothermic peak in the DSC heating curve indicated the development of metastable situation upon cooling. Presumably a part of the water solidified in an amorphous state during the cooling process (Yoshida, 1991; Aoki et al., 1995), and this water crystallized during the heating process. It seems that the faint endothermic peak represent melting of imperfect water crystals attributed to the interaction between NS, HPMC and water. Such behavior was not observed in NS solutions without the polymer. A similar effect of NS on bound water was found in EA + NS system, however protein hydration was additionally influenced by protein unfolding and water crystallization was not observed (unpublished data).

Fig. 8a presents the freezing and non-freezing water per dry sample in the outer surface of hydrated HPMC/NS matrices of various viscosity grades. The ratio of freezing water per dry sample was higher for higher viscosity grade (MW) of the polymer (K100M > K4M > K100LV). The average ratio of non-freezing water (mol) per PRU for K100LV, K4M and K100M hydrated matrices was 4.320 ± 1.011, 5.317 ± 1.454 and 5.039 ± 1.224, respectively. The DSC graph shape of

freezable water in the outer gel layer of the matrices (Fig. 9) show a faint endotherm below 0°C, similar to that observed with HPMC K4M + NS samples. Fig. 8b show that up to 8 h freezable water was not detected in the inner portion of the matrices. Above 8 h, the amount of freezable water in the center of the matrices increased. The penetration rate for HPMC (K4M) was slightly higher compared to K100M. This can be explained by the higher swelling (data not shown) of K100M matrices, which retarded the hydration of the inner core. For HPMC K4M and K100M matrices, the ratio of freezable water (per dry sample) at the surface increased after 8 h. The results indicate that amount of freezable water per dry sample in the gelatinized surface layer of the matrix did not increase until the whole matrix was hydrated which is in agreement with the results reported by Aoki et al., for the hydration of hydroxypropylcellulose and ethyl cellulose matrices. The constant amount of freezable water per dry sample for K100LV matrices supported the surface erosion mechanism of the matrix. For matrices undergoing bulk erosion mechanism (for example 100% EA matrices) this ratio increases as matrix erosion proceeds (unpublished data). The results imply that HPMC matrices of higher viscosity grades (higher MW) are characterized by higher ratio of freezable water per dry sample. The higher water absorption capacity of higher HPMC viscosity grades led to increase of matrix swelling and to decrease in the differences of hydrated matrix microviscosity values for the three MW of HPMC. These effects lead to similar diffusional drug release profiles for high MW of HPMC (K4M, K100M) with slightly higher release for K4M. Regarding K100LV matrices, although drug diffusion is anticipated to be similar based on the microviscosity values, the higher erosion (polymer disentanglement) of K100LV matrices increased drug release significantly.

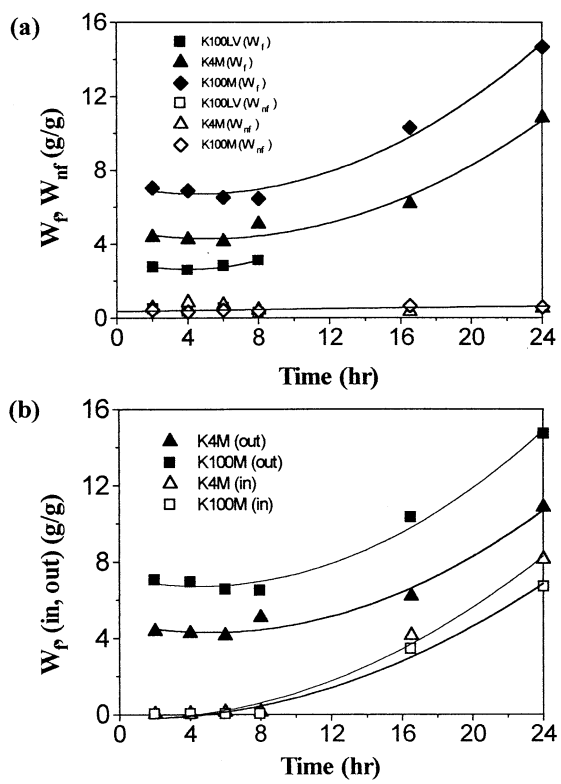

Fig. 8. (a) Freezing and non-freezing water per dry sample in the outer surface of HPMC/NS matrices; (b) Freezing water per dry sample in the inner core of HPMC/NS matrices compared with the outer surface.

4. Conclusions

From the data obtained here it can be concluded that matrices composed of various viscosity grades of HPMC are characterized by similar microviscosity values in spite of the difference in their molecular weight. The NMR and DSC results led to the conclusion that higher molecular weights of HPMC are characterized by higher water absorption capacity and higher swelling. Analysis of non-freezable water in HPMC(K4M)-NS system revealed that addition of NS to solution increased the fraction of water bound to K4M + NS compared with the equivalent solutions without NS. The results suggest that the drug is participating in the crystallization of water and leads to the formation of a three dimensional network structure that decreases the freedom of water in K4M + NS samples. It was found (based on DSC data) that 2.2 hydration layers are involved in K4M-NS hydration compared with 1.5 for HPMC gel without the drug. This was explained based on the different water ordering in

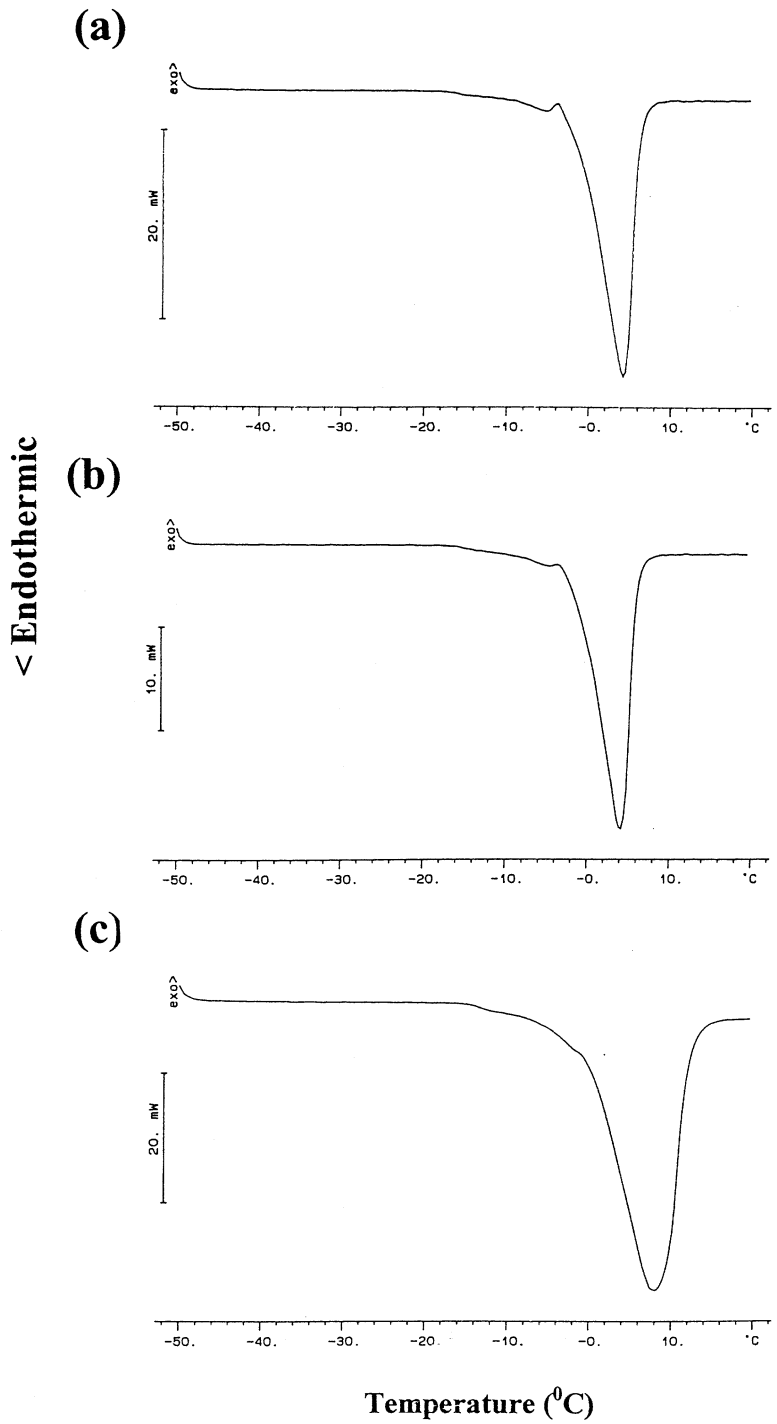

Fig. 9. DSC thermographs of samples taken from the outer surface of HPMC(K4M)/NS matrices at various hydration intervals. (a) 2 h; (b) 6 h; (c) 16 h.

the gel induced by NS as a result of its absorption to polymer surface. Microviscosity values measured by EPR for K4M/N and K4M/NS hydrated matrices were found to be higher for K4M/N matrices, especially at initial stage of hydration. Mobile compartment calculations showed lower values for K4M/N compared with K4M/NS matrices. pH measurements by EPR revealed that incorporation of N to HPMC matrix led to lower internal pH value inside the hydrated tablet compared with NS in which this value was closer to the penetrating buffer, pH 7.4. This behavior leads to lower solubility of N, which dictates its surface erosion mechanism, compared with NS matrix, which was characterized by higher internal pH value and higher drug solubility. These properties of HPMC/NS increased chain hydration and stability, and led to drug release by the diffusion mechanism.

Acknowledgements

The authors wish to thank Dr Aba Priev, Department of Biochemistry, Faculty of Medicine, The Hebrew University of Jerusalem for valuable discussions and helpful comments.

References

Alderman, D.A., 1984. A review of cellulose ethers in hydrophilic matrices for oral controlled-release dosage forms. Int. J. Pharm. Tech. Prod. Man. 5, 1–9.

Angell, C.A., Tucker, J.C., 1973. Anomalous heat capacities of supercooled water and heavy water. Science 181, 342–344.

Aoki, S., Ando, H., Ishii, M., Watanabe, S., Ozawa, H., 1995. Water behavior during drug release from a matrix as observed using differential scanning calorimetry. J. Control. Rel. 33, 365–374.

Berliner, L.J., 1976. Spin Labeling: Theory and Applications. Academic Press, New York.

Bondi, A., 1968. Physical Properties of Molecular Crystals, Liquids and Gasses. Wiley, New York, pp. 450–469.

Chalikian, T.V., Sarvazian, A.P., Breslauer, K.J., 1994. Hydration and partial compressibility of biological compounds. Biophys. Chem. 51, 89–109.

Cotts, R.M., Hoch, M.J.R., Sun, T., Markert, J.T., 1989. Pulsed field gradient stimulated echo methods for improved NMR diffusion measurements in heterogeneous systems. J. Magn. Reson. 83, 252–266.

Derome, A.E., 1987. Modern NMR techniques for chemistry research. In: Baldwin, J.E. (Ed.) Organic Chemistry Series; vol 6. Pergamon Press, Oxford.

Ford, J.L., Rubinstein, M.H., McCaul, F., Hogan, J.E., Edgar, P.J., 1987. Importance of drug type, tablet shape and added diluents on drug release kinetics from hydroxypropylmethylcellulose matrix tablets. Int. J. Pharm. 40, 223–234.

Fyfe, C.A., Blazek, A.I., 1997. Investigation of hydrogel formation from hydroxypropylmethylcellulose (HPMC) by NMR spectroscopy and NMR imaging techniques. Macromolecules 30, 6230–6237.

Gao, P., Fagerness, P.E., 1995. Diffusion in HPMC gels. I. Determination of drug and water diffusivity by pulsed-field-gradient spin-echo NMR. Pharm. Res. 12, 955–964.

Hatakeyama, H., Yamauchi, A., 1984. Studies on bound water in poly (vinyl alcohol) hydrogel by DSC and FT-NMR. Eur. Polym. J. 1, 61–64.

Hodsdon, A.C., Mitchel, J.R., Davies, M.C., Melia, C.D., 1995. Structure and behaviour in hydrophilic matrix sustained release dosage forms: 3. The influence of pH on the sustained release performance and internal gel structure of sodium alginate matrices. J. Control. Rel. 33, 143–152.

Joshi, H.N., Topp, E.M., 1992. Hydration in hyaluronic acid and in esters using differential scanning calorimetry. Int. J. Pharm. 80, 213–225.

Katzhendler, I., Mäder, K., Azoury, R., Friedman, M., 1999. Investigating the structure and properties of hydrated hydroxypropyl methylcellulose and egg albumin matrices containing carbamazepine: EPR and NMR study. Submitted for publication.

Katzhendler, I., Mäder, K., Friedman, M., 2000. Correlation between drug release kinetics from proteineous matrix and matrix structure: EPR and NMR study. J. Pharm. Sci. 89, 365–381.

Kharakoz, D.P., 1991. Volumetric properties of proteins and their analogs in diluted water solutions. 2. Partial adiabatic compressibilities of amino acids at 15–700C. J. Phys. Chem. 95, 5634–5642.

Mäder, K., Swartz, H.M., Stösser, R., Borchert, H.H., 1994. The application of EPR spectroscopy in the field of pharmacy. Pharmazie 49, 97–101.

Mathur-De Vre, R., 1979. The NMR studies of water in biological systems. Prog. Biophys. Mol. Biol. 35, 103–134.

Melia, C.D., 1991. Hydrophilic matrix sustained release systems based on polysaccharide carriers. Crit. Rev. Ther. Drug Carrier Syst. 8, 395–421.

Melia, C.D., Binns, J.S., Davies, M.C., 1990. Polymer hydration and drug distribution within the gel layer of hydrophilic matrix devices during drug release. J. Pharm. Pharmacol. 42, 125P.

Melia, C.D., Hodsdon, A.C., Davies, M.C., Mitchell, J.R., 1994. Polymer concentration profiles of the surface gel layer of xanthan, alginate and HPMC matrix systems. Proc. Int. Symp. Control. Rel. Bioact. Mater. 21, 724–725.

Nakamura, T., Hatakeyaka, T., Hatakeyaka, H., 1983. Effect of bound water on tensile properties of native cellulose derivatives. Text. Res. J. 53, 1017–1024.

Nordio, P.L., 1976. In: Berliner, L.J. (Ed.), Spin Labeling: Theory and Applications, Academic Press, New York, p. 34.

Ohno, H., Shibayama, M., Tsuchida, E., 1983. DSC Analyses of bound water in the microdomains of interpolymer complexes. Macromol. Chem. 184, 1017–1024.

Phillies, G.D.J., 1987. Dynamics of polymers in concentrated solutions; the universal scaling equation derived. Macromolecules 20, 558–564.

Phillies, G.D.J., 1988. Quantitative prediction of alpha in the scaling law for self-diffusion. Macromolecules 21, 3101–3106.

Rajabi-Siahboomi, A.R., Bowtell, R.W., Mansfield, P., Davis, M.C., Melia, C.D., 1996. Structure and behavior in hydrophilic matrix sustained release dosage forms: 4. Studies of water mobility and diffusion coefficients in the gel layer of HPMC tablets using NMR imaging. Pharm. Res. 13, 376–380.

Roorda, W.E., Bouwsta, J.A., Junginger, H.E., 1988. Thermal behavior of poly hydroxy ethyl methacrylate (pHEMA) hydrogels. Pharm. Res. 5, 722–725.

Stilbs, P., 1987. Fourier transform pulsed-gradient spin-echo studies of molecular diffusion. Prog. NMR Spectrosc. 19, 1–45.

Stösser, R., Mäder, K., Borchert, H.H., Herrmann, W., Schneider, G., Leiro, W.A., 1995. In: Ohya-Nishiguchi, H., Packer, L. (Ed.), Bioradicals Detected by ESR Spectroscopy. Birkhauser Verlag, Basel, pp. 301–320.

Tanner, J.E., 1970. Use of the stimulated echo in NMR diffusion studies. J. Chem. Phys. 52, 2523–2526.

Touitou, E., Donbrow, M., 1982. Influence of additives on (hydroxyethyl) methylcellulose properties: relation between gelation temperature change, compressed matrix integrity and drug release profile. Int. J. Pharm. 11, 131–148.

US Pharmacopea XXI, 1985. US Pharmacopeial Convention, Rockville, MD, p 1420.

Weast, R.C., Astle, M.C., Beyer, W.H., 1986/87. CRC Handbook of Chemistry and Physics; FL, CRS Press, Boca Raton.

Wertz, J.E., Bolton, J.R., 1972. Electron Spin Resonance: Elementry Theory and Practical Applications. McGraw Hill, New York.

Yoshida, H., 1991. Effect of amorphous ice on the glass transition of frozen gel. Netsu Sokutei 18, 240–241.